Lipocalin-2 Deficiency Impairs Thermogenesis and Potentiates Diet-Induced Insulin Resistance in Mice

Hong Guo,[1] Daozhong Jin,[1] Yuanyuan Zhang,[1] Wendy Wright,[2] Merlijn Bazuine,[3] David A. Brockman,[1] David A. Bernlohr,[2] and Xiaoli Chen[1]

OBJECTIVE—Lipocalin (LCN) 2 belongs to the lipocalin subfamily of low–molecular mass–secreted proteins that bind small hydrophobic molecules. LCN2 has been recently characterized as an adipose-derived cytokine, and its expression is upregulated in adipose tissue in genetically obese rodents. The objective of this study was to investigate the role of LCN2 in diet-induced insulin resistance and metabolic homeostasis in vivo.

RESEARCH DESIGN AND METHODS—Systemic insulin sensitivity, adaptive thermogenesis, and serum metabolic and lipid profile were assessed in LCN2-deficient mice fed a high-fat diet (HFD) or regular chow diet.

RESULTS—The molecular disruption of LCN2 in mice resulted in significantly potentiated diet-induced obesity, dyslipidemia, fatty liver disease, and insulin resistance. *LCN2*$^{-/-}$ mice exhibit impaired adaptive thermogenesis and cold intolerance. Gene expression patterns in white and brown adipose tissue, liver, and muscle indicate that *LCN2*$^{-/-}$ mice have increased hepatic gluconeogenesis, decreased mitochondrial oxidative capacity, impaired lipid metabolism, and increased inflammatory state under the HFD condition.

CONCLUSIONS—LCN2 has a novel role in adaptive thermoregulation and diet-induced insulin resistance. ***Diabetes* 59:1376–1385, 2010**

Obesity is a major risk for developing insulin resistance, a hallmark of type 2 diabetes and other metabolic complications such as fatty liver, dyslipidemia, and atherosclerosis. Adipose tissue plays a central role in body weight homeostasis, inflammation, and insulin resistance via regulating lipid metabolism/storage and releasing a range of adipokines/cytokines (1–4). Adipose tissue in a variety of insulin-resistant states has been characterized by dysregulated lipid metabolism and altered production of adipokines/cytokines that, in sum, are important contributors to systemic inflammation and related metabolic disorders.

Lipocalin (LCN) 2 (also known as neutrophil gelatinase–associated lipocalin [NGAL]), a lipocalin subfamily member, has been recently identified by our group and others (5,6) as an adipose-derived cytokine. LCN2 is a 25-kDa secreted protein initially identified from human neutrophils (7,8) and other immune cells and tissues that are exposed to microorganisms in the respiratory and gastrointestinal tract and is present abundantly in the circulation (9). Interestingly, lipocalins have structural similarity with fatty acid binding proteins (FABPs), and both are members of the multigene family of up and down β-barrel proteins (10). Both the intracellular FABPs and the extracellular lipocalins have a clearly defined β-barrel motif that forms either an interior cavity (FABP) or a deep pit (lipocalins) that constitutes the lipid binding domain (10). The extracellular lipocalins such as LCN2, retinol binding protein (RBP) 4, and α_2-microglobulin use a series of β-strands to form a globular domain with a deep depression resembling the calyx of a flower. Because of the unique structure, the lipocalins function as efficient transporters for a number of different hydrophobic ligands in extracellular milieus, including a variety of retinoids, fatty acids, biliverdin, pheromones, porphyrins, odorants, steroids, and iron. RBP4, one of the extracellular lipocalins, affects glucose metabolism and insulin sensitivity (11).

Previous studies have demonstrated that *LCN2* gene expression is upregulated in adipose tissue and liver of genetically obese animals (6). Rosiglitazone administration significantly reduces LCN2 expression in adipose tissue in obese animals (6), suggesting that the protein may function as a proinflammatory factor. Unexpectedly, the addition of LCN2 protein to the culture media of adipocytes and macrophages leads to the suppression of tumor necrosis factor (TNF)α- and lipopolysaccharide-induced cytokine/chemokine production, indicating an anti-inflammatory function (6). Most strikingly, LCN2 appears to protect against TNFα-induced insulin resistance in adipocytes. Unlike RBP4, increased production of LCN2 in obesity may be a protective mechanism against inflammation and insulin resistance.

To evaluate this hypothesis, we assessed the metabolic and regulatory consequences of LCN2 deficiency. Herein, we show that the ablation of LCN2 profoundly impairs adaptive thermogenesis and exacerbates high-fat diet (HFD)- or age-induced insulin resistance and glucose homeostasis. LCN2-deficient mice have increased hepatic gluconeogenesis and inflammatory state and exhibit a cold sensitive phenotype.

RESEARCH DESIGN AND METHODS

LCN2$^{-/-}$ mice were kindly provided by Dr. Alan Aderem (Institute for Systems Biology, Seattle, Washington), which were originally generated by Dr. Shizuo Akira (Research Institute for Microbial Diseases, Osaka University, Osaka, Japan). *LCN2*$^{-/-}$ mice were generated by gene targeting in embryonic

From the [1]Department of Food Science and Nutrition, University of Minnesota, Minneapolis–St. Paul, Minnesota; the [2]Department of Biochemistry, Molecular Biology and Biophysics, University of Minnesota, Minneapolis–St. Paul, Minnesota; and the [3]Experimental Diabetes, Metabolism, and Nutrition Section, Diabetes Branch, National Institute of Diabetes and Digestive and Kidney Diseases, National Institutes of Health, Bethesda, Maryland.

Corresponding author: Xiaoli Chen, xlchen@umn.edu.

Received 25 November 2009 and accepted 8 March 2010. Published ahead of print at http://diabetes.diabetesjournals.org on 23 March 2010. DOI: 10.2337/db09-1735.

H.G., D.J., and Y.Z. equally contributed to this work.

© 2010 by the American Diabetes Association. Readers may use this article as long as the work is properly cited, the use is educational and not for profit, and the work is not altered. See http://creativecommons.org/licenses/by-nc-nd/3.0/ for details.

The costs of publication of this article were defrayed in part by the payment of page charges. This article must therefore be hereby marked "advertisement" in accordance with 18 U.S.C. Section 1734 solely to indicate this fact.

stem (ES) cells from mouse strain 129, and targeted ES cells were injected into C57BL/6 blastocysts as described previously (12). C57BL/6 mice were purchased from The Jackson Laboratory (Bar Harbor, ME). LCN2-null mice were backcrossed onto the B6 background for 10 generations before mice were used for the experiments. Heterozygous mating scheme was used to generate wild-type and *LCN2*$^{-/-}$ mice for the experiments.

Aminals were housed in a specific pathegon-free facility at the University of Minnesota. Animal handling followed the National Institutes of Health guidelines, and experimental procedures were approved by the University of Minnesota Animal Care and Use Committee. Age-matched male wild-type and *LCN2*$^{-/-}$ mice were allocated into groups (3–4 mice/cage) and fed an HFD (fat calories: 60%) obtained from Bio-Serv (F3282; New Brunswick, NJ) or a regular chow diet (RCD), with free access to water for all studies. In the adaptive thermogenesis study, age-matched wild-type and *LCN2*$^{-/-}$ mice on an RCD were exposed to 4°C, with free acess to diet and water. Rectal temperature of the mice was measured at the indicated time points using a MicroTherma Thermometer with rectal probe for mice (Braintree Scientific, Braintree, MA).

Metabolic studies. During the experiemental period of HFD feeding, glucose and insulin tolerance tests were conducted by the intraperitoneal injection of glucose and insulin. Mice were fasted overnight (12 h) for the glucose tolerance test (GTT) and for 6 h for insulin tolerance tests (ITTs). GTTs and ITTs were conducted by intraperitoneal injection of glucose (1 mg/g body wt) or insulin (0.75 units/kg body wt) with blood collection via the tail vein at 0, 15, 30, 60, 90, and 120 min. Blood glucose was measured using an Ascensia glucometer.

Triglyceride content measurement. Lipid extraction was performed using the Bligh-Dyer method (13). Briefly, frozen liver tissue (100 mg) was homogenized in 1 ml water. Lipid was extracted using chloroform:methanol (2:1). An aliquot of the organic phase was collected and dried with nitrogen and then dissolved in isopropanol alcohol containing 1% Triton. Triglyceride content was determined using commercially available kits (Stanbio Lab, reference no. 2150-1).

Primary mouse adipose cell isolation. Preparation of isolated adipose cells from wild-type and *LCN2*$^{-/-}$ mice was performed as described previously (14,15). After mincing, epididymal fat pads were digested with collagenase (2 mg/ml solution) in digestion vials containing Krebs-Ringer bicarbonate HEPES buffer, pH 7.4; 200 nmol/l adenosine; and 3.5% BSA. After a 2-h digestion, adipose cells were separated by centrifugation at 1,200 rpm for 10 min and washed twice with Krebs-Ringer bicarbonate HEPES buffer. After the final wash, adipose cells were collected for RNA extraction.

Adipose cell size analysis. Adipose tissue was obtained from the epididymal and inguinal fat pad of wild-type and *LCN2*$^{-/-}$ mice fed an RCD. Tissue samples (20–30 mg) were immediately fixed in osmium tetroxide and incubated in a water bath at 37°C for 48 h, as described previously (16), and then adipose cell size was determined by a Beckman Coulter Multisizer III with a 400-μm aperture. The range of cell sizes that can effectively be measured using this aperture is 20–240 μm. After collection of pulse sizes, the data were expressed as particle diameters and displayed as histograms of counts against diameter using linear bins and a linear scale for the x-axis. The figures were generated using GraphPad Prism 5.01 for Windows (GraphPad Software, La Jolla, CA).

Statistical analysis. Results were expressed as means ± SE. Differences in parameters between wild-type and *LCN2*$^{-/-}$ mice were evaluated using a two-group *t* test with a 0.05 two-sided significance level. A *P* value <0.05 was considered significant.

RESULTS

***LCN2*$^{-/-}$ mice are more susceptible to diet-induced obesity.** At 3 weeks of age, male wild-type and LCN2$^{-/-}$ mice were fed either an HFD for 12 weeks or RCD. Throughout the experimental period, body weight was significantly different between wild-type and *LCN2*$^{-/-}$ mice fed an HFD (Fig. 1*A*) and RCD (Fig. 1*B*). *LCN2*$^{-/-}$ mice were significantly heavier than wild-type mice on either an HFD or RCD. The weight of white and brown fat pads was significantly higher in HFD-fed (Fig. 1*C*) or aged *LCN2*$^{-/-}$ (Fig. 1*D*) mice than that in wild-type mice. Both HFD-fed and aged *LCN2*$^{-/-}$ mice showed a significantly higher weight of liver, heart, kidney, and spleen (Fig. 1*E* and *F*). Similar metabolic phenotypes were also observed in female *LCN2*$^{-/-}$ mice (data not shown). However, the overall growth did not appear to be significantly affected, as the body length and bone length (trabecular) were not significantly different between the genotypes (data not shown). Figure 1*G* and *H* demonstrated the fat-cell size distributions of wild-type and *LCN2*$^{-/-}$ mice on an RCD at 15 weeks of age, as measured by Multisizer analysis using cells isolated from osmium-fixed epididymal and inguinal adipose tissue. The average peak diameter of the large-cell population was significantly larger for *LCN2*$^{-/-}$ mice compared with wild-type mice, indicating that *LCN2*$^{-/-}$ adipose tissue contains larger adipose cells.

***LCN2*$^{-/-}$ mice display impaired adaptive thermogenesis.** Because LCN2-deficient mice gained more body weight and increased adiposity, particularly when mice were fed an HFD or aged, we examined food intake and energy expenditure in *LCN2*$^{-/-}$ mice. An analysis of indirect calorimetry measurements showed that food intake, ambulatory activity, V_{O_2}, and R_Q were not significantly different between RCD-fed wild-type and *LCN2*$^{-/-}$ mice at 18 weeks of age (Fig. S1 in the online appendix, available at http://diabetes.diabetesjournals.org/cgi/content/full/db09–1735/DC1). We then assessed thermogenic activity of brown adipose tissue (BAT) under thermoneutral and thermal stress conditions. Body temperature was measured in an ambient temperature of 28°C and 22°C as well as during acute exposure to 4°C. Wild-type and *LCN2*$^{-/-}$ mice at 12 weeks of age exhibited a similar body temperature in an ambient temperature of 28°C (wild type, 38.34 ± 0.34; *LCN2*$^{-/-}$, 38.2 ± 0.30). However, female *LCN2*$^{-/-}$ mice had a significantly lower rectal temperature than wild-type mice (Fig. 2*A*), while male *LCN2*$^{-/-}$ mice had a trend toward decrease in rectal temperature when kept in an ambient temperature of 22°C. More strikingly, *LCN2*$^{-/-}$ mice displayed cold sensitivity and could not survive when exposed to 4°C for >10 h. *LCN2*$^{-/-}$ mice (seven of seven) died after being exposed to 4°C for 12 h, while all of the wild-type mice (n = 7) in the experiment survived. When acutely exposed to 4°C, rectal temperature of *LCN2*$^{-/-}$ mice dropped significantly within 3 h compared with wild-type mice (Fig. 2*B*). Five-hour cold exposure caused a 10-fold increase in *LCN2* gene expression in adipose tissue in wild-type mice (Fig. 2*C*), suggesting that LCN2 is a critical regulator of energy metabolism.

To explore the possible mechanisms for cold intolerance in *LCN2*$^{-/-}$ mice, uncoupling protein (UCP)-1–mediated thermogenic activity and capacity of BAT was first evaluated under the conditions of HFD feeding and cold exposure. We observed that upon HFD feeding, *LCN2*$^{-/-}$ mice expressed significantly lower levels of *UCP-1* and peroxisome proliferator–activated receptor (*PPAR*) γ coactivator (*PGC-1*)α genes in BAT than wild-type mice mice (Fig. 2*D*). However, *UCP-1* and *PGC-1*α expression in BAT were markedly stimulated at an even higher level in *LCN2*$^{-/-}$ mice, as wild-type mice after exposure to 4°C for 5 h (Fig. 2*E*). This suggests that *LCN2*$^{-/-}$ BAT remains at normal UCP-1–dependent thermogenic activity. We next examined whether the regulation of substrate provision is altered in *LCN2*$^{-/-}$ mice. Figure 2*F* showed that the protein expression levels of adipose triglyceride lipase (ATGL) in white adipose tissue (WAT) were slightly reduced in *LCN2*$^{-/-}$ mice under the HFD and cold condition compared with wild-type mice. However, cold-induced *HSL* gene expression in BAT and WAT was completely diminished in *LCN2*$^{-/-}$ mice (Fig. 2*G*). Lastly, we investigated the mitochondrial oxidative capacity of BAT, as this function of BAT is critical for providing the energy for thermogenesis. Interestingly, we observed that there

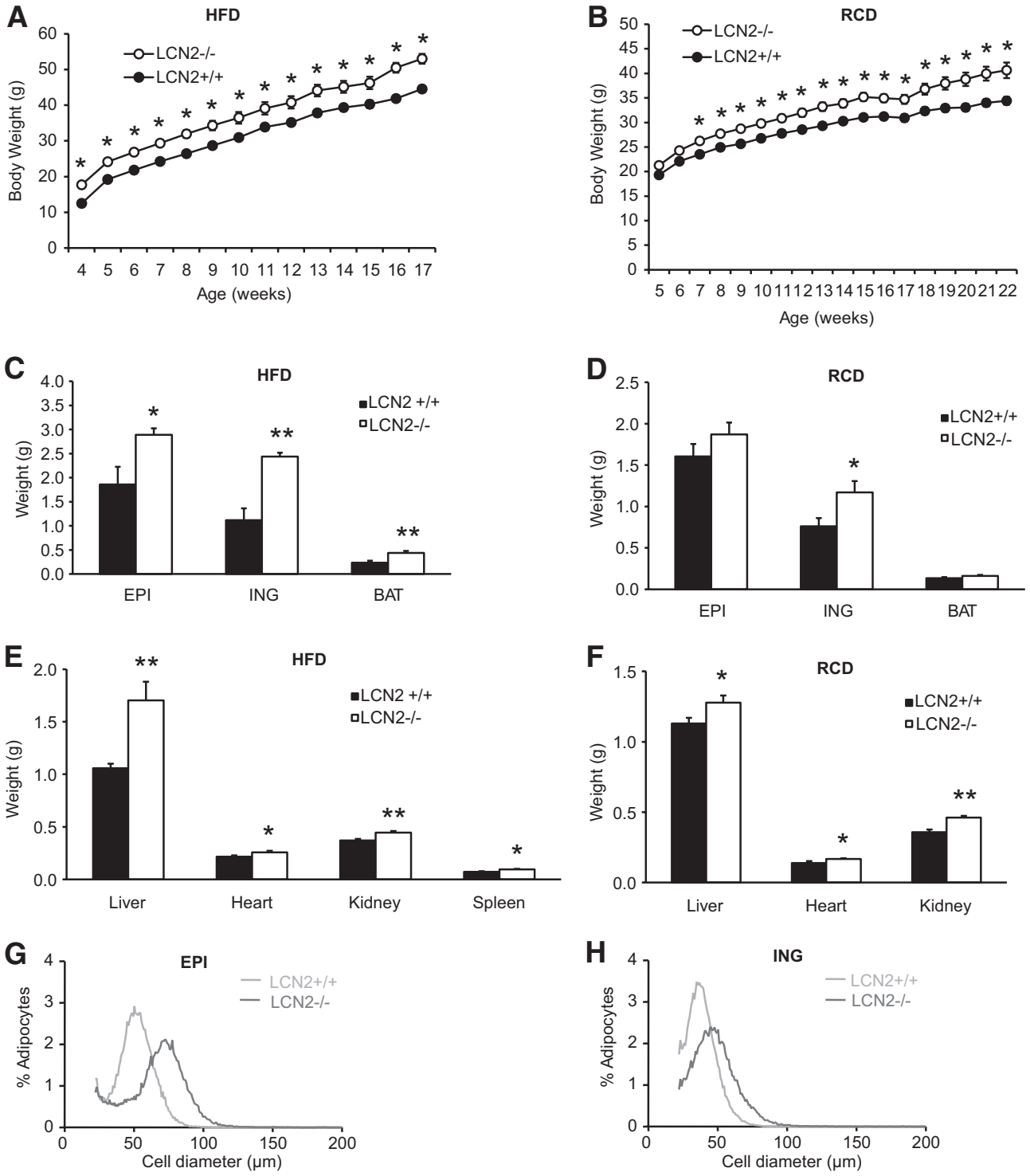

FIG. 1. Growth curve, weight of white and brown fat pads and organs in *LCN2*$^{-/-}$ mice. Growth curve of *LCN2*$^{-/-}$ mice on an HFD (n = 10–14) (*A*) and RCD (n = 13) (*B*). Fat pad weight of *LCN2*$^{-/-}$ mice on an HFD at 16 weeks of age (*C*) and on RCD at 30 weeks of age (*D*). Organ weight of *LCN2*$^{-/-}$ mice on HFD at 16 weeks of age (*E*) and on RCD at 30 weeks of age (*F*). The data are represented as mean ± SE. *P < 0.05; **P < 0.01. Fat-cell size distribution of mice on RCD diet at 15 weeks of age (*G* and *H*). EPI: epididymal; ING: inguinal.

was a significant reduction in the expression levels of mitochondrial genes involved in mitochondrial biogenesis and oxidative function, such as nuclear respiratory factor (*Nrf*)1, transcription factor A, mitochondrial (*Tfam*), ATP synthase 5β (*ATP5β*), cytochrome c oxidase (*COX*) 4, and carnitine palmitoyltransferase (*CPT*)-1β in BAT of *LCN2*$^{-/-}$ mice fed an HFD (Fig. 2*H*). In addition, the expression of transcription factors *PPARδ*, *Nrf1* and *Tfam*, and *CPT-1* gene in skeletal muscle was also significantly downregulated in *LCN2*$^{-/-}$ mice fed an HFD (Fig. 2*D*).

***LCN2*$^{-/-}$ mice develop more severe diet-induced insulin resistance and increased inflammatory state.** To assess the effects of LCN2 deficiency on systemic insulin sensitivity, GTTs and ITTs were performed. Glucose clearance curves in response to glucose administration were significantly increased in HFD-fed (Fig. 3*A*) but

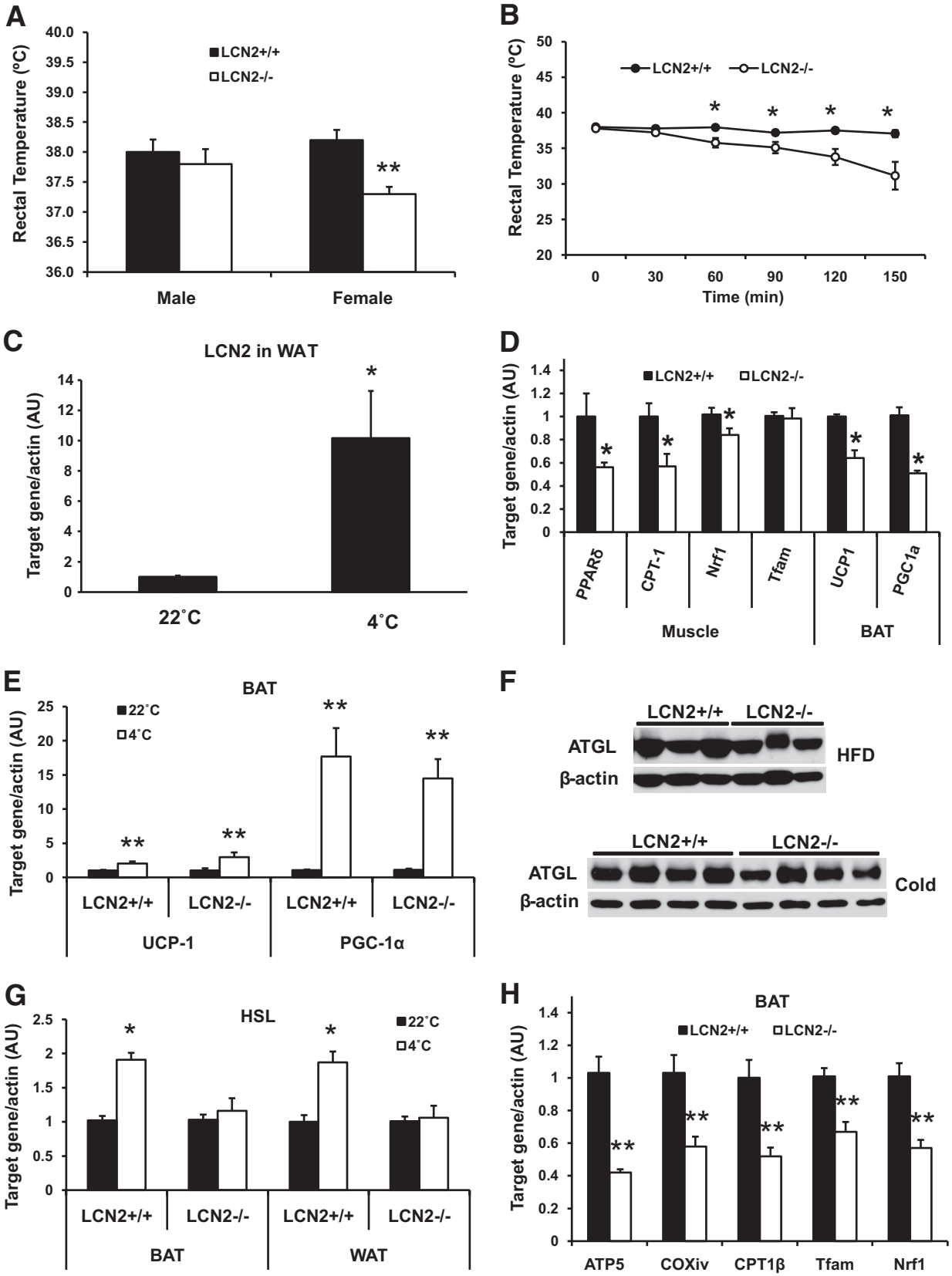

FIG. 2. Adaptive thermogenesis in *LCN2*$^{-/-}$ mice. *A*: Basal rectal body temperature of 8-week-old male and female wild-type and *LCN2*$^{-/-}$ mice on an RCD (n = 7–10) measured during the daytime in an ambient temperature of 22°C. *B*: Body temperature curve of *LCN2*$^{-/-}$ mice (n = 8) and wild-type mice (n = 7) exposed to 4°C. *C*: Gene expression of *LCN2* in WAT of wild-type mice exposed to 4°C for 5 h. *D*: Gene expression of *UCP-1* and *PGC-1α* in BAT and *PPARδ*, *CPT-1*, *Tfam*, and *Nrf1* in skeletal muscle of HFD-fed mice (n = 6). *E*: Gene expression of *UCP-1* and *PGC-1α* in BAT. *F*: ATGL protein expression in WAT under the HFD and cold conditions. *G*: Gene expression of *HSL* in BAT and WAT of mice exposed to 4°C for 5 h. *H*: Gene expression of mitochondrial genes in BAT of LCN2$^{-/-}$ mice under the HFD condition. The data are represented as means ± SE. *P < 0.05; **P < 0.01.

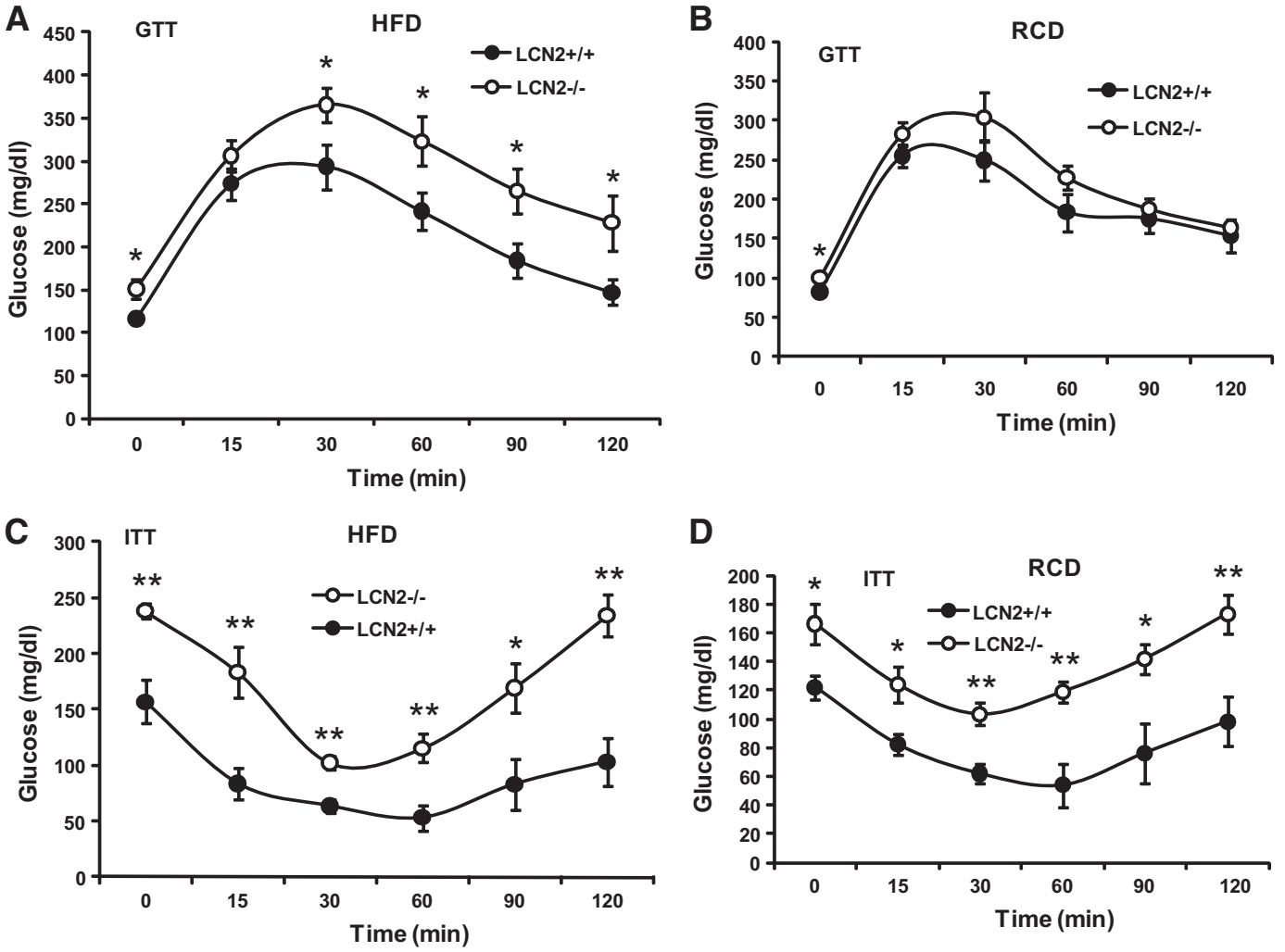

FIG. 3. Assessment of insulin sensitivity. GTTs (*A*) and ITTs (*C*) conducted in *LCN2*$^{-/-}$ mice on an HFD (n = 10–12, age 14–15 weeks). GTTs (*B*) and ITTs (*D*) conducted in *LCN2*$^{-/-}$ mice on an RCD (n = 10–12, age 28–29 weeks). Data are represented as means ± SE. Experiments were repeated on two independent sets of mice, yielding similar results. *P < 0.05; **P < 0.01.

not RCD-fed *LCN2*$^{-/-}$ mice (Fig. 3*B*), indicating that *LCN2*$^{-/-}$ mice are more glucose intolerant upon HFD feeding. In the ITT, increased insulin-stimulated glucose disposal curve was observed in *LCN2*$^{-/-}$ mice, indicating that *LCN2*$^{-/-}$ mice are more insulin resistant than wild-type controls when fed an HFD (Fig. 3*C*) or aged (Fig. 3*D*). Analysis of serum metabolic parameters, as shown in Table 1, demonstrated that levels of fasting serum glucose and insulin were significantly elevated, while adiponectin levels were reduced in HFD-fed *LCN2*$^{-/-}$ mice when compared with wild-type controls. Serum levels of leptin and plasminogen activator inhibitor-1 were not significantly changed in *LCN2*$^{-/-}$ mice on an RCD, although serum leptin levels had a trend toward a decrease in HFD-fed *LCN2*$^{-/-}$ mice. After adjustment to body weight, the serum levels of glucose, insulin, and adiponectin were consistently different at the statistically significant level, indicating that the changes in glucose tolerance and insulin sensitivity after HFD in *LCN2*$^{-/-}$ mice is not simply due to body weight effects. To further confirm that *LCN2*$^{-/-}$ mice have decreased insulin sensitivity, in vivo insulin-stimulated Akt phosphorylation was evaluated.

TABLE 1
Serum metabolic parameters in wild-type and *LCN2*$^{-/-}$ mice

Genotype	Diet	Glucose (mg/ml)	Insulin (ng/ml)	Leptin (ng/ml)	Adiponectin (μg/ml)	Plasminogen activator inhibitor-1 (ng/ml)
Wild type	RCD	82.33 ± 3.27	0.56 ± 0.15	3.33 ± 1.56	14.78 ± 1.85	3.59 ± 0.51
LCN2$^{-/-}$	RCD	100.38 ± 4.99*	0.79 ± 0.11	3.06 ± 0.95	15.46 ± 1.02	3.22 ± 0.62
Wild type	HFD	157.10 ± 19.55	1.85 ± 0.36	24.23 ± 3.86	16.50 ± 0.34	2.83 ± 0.42
LCN2$^{-/-}$	HFD	238.13 ± 6.45†	3.02 ± 0.57†	16.62 ± 2.07	13.50 ± 0.88†	3.43 ± 0.79

Data are means ± SE. Measurements were performed on 6-h–fasted mice fed an RCD and HFD (n = 9–11). *P < 0.01 vs. wild-type on an RCD; †P < 0.01 vs. wild-type on an HFD.

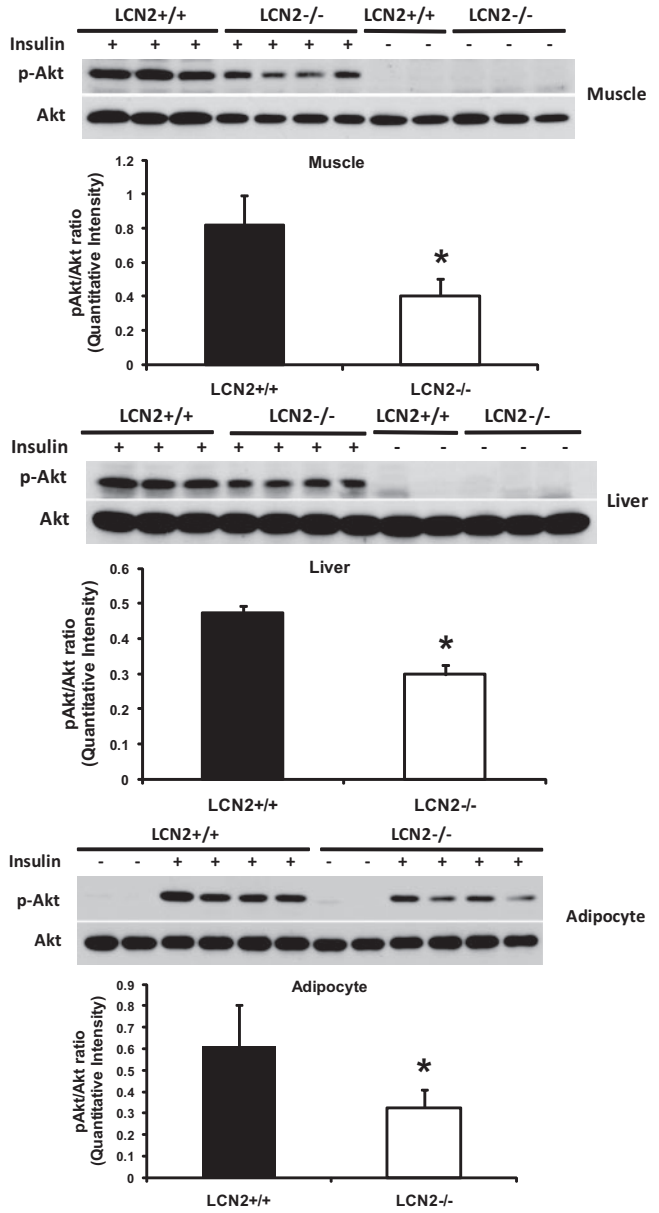

FIG. 4. In vivo insulin-stimulated Akt phosphorylation in *LCN2*$^{-/-}$ mice. Representative Western blot analysis of serine-phosphorylated Akt in muscle, liver, and isolated primary adipose cells from *LCN2*$^{-/-}$ (n = 4 per group) and wild-type mice (n = 4 per group) under basal and in vivo insulin-stimulated conditions.

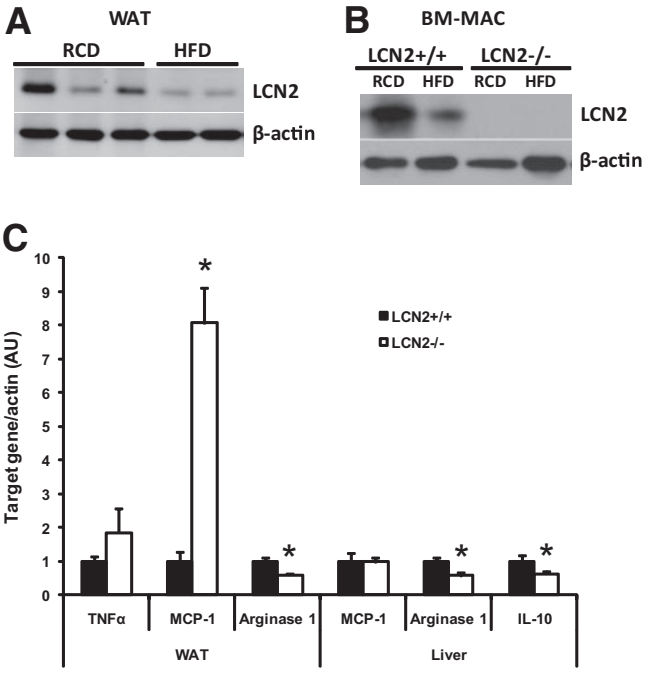

FIG. 5. Protein expression levels of *LCN2* and gene expression of proinflammatory molecules in LCN2$^{-/-}$ mice. *A*: Protein expression levels of LCN2 in adipose tissues of wild-type mice fed an RCD and HFD. *B*: Protein expression levels of LCN2 in bone marrow macrophages (BM-MAC) isolated from wild-type mice fed an RCD and HFD. *C*: Gene expression of inflammatory molecules in adipose tissue and liver of wild-type and *LCN2*$^{-/-}$ mice fed on HFD. The data of gene expression are represented as means ± SE. *P < 0.05.

Wild-type and *LCN2*$^{-/-}$ mice on RCD were injected intraperitoneally with insulin, killed after 10 min, and tissues were collected for evaluation of Akt phosohorylation. Consistently, insulin-stimulated Akt phosphorylation in liver, muscle, and adipose cells was significantly reduced in *LCN2*$^{-/-}$ mice as compared with wild-type mice (Fig. 4). The examination of LCN2 effect on upstream signaling components of insulin signaling pathway demonstrated that the expression levels of insulin receptor substrate-1 protein were markedly reduced in WAT of *LCN2*$^{-/-}$ mice on an HFD compared with wild-type mice (Fig. S2). This data further support that *LCN2*$^{-/-}$ mice developed more insulin resistance and LCN2 regulates insulin signaling activity likely at the upstream level.

To test the role of LCN2 in inflammatory response, expression of LCN2 and inflammatory molecules was examined in adipose tissue and liver of HFD-induced wild-type and *LCN2*$^{-/-}$ mice. The protein expression levels of LCN2 were decreased in adipose tissue (Fig. 5*A*) and bone marrow–derived macrophages of normal mice upon an HFD feeding (Fig. 5*B*). Furthermore, the gene expression of proinflammatory cytokine *TNFα* and monocyte chemoattractant protein (*MCP*)-*1* were upregulated, while expression of arginase 1, an anti-inflammatory marker, was downregulated in adipose tissue of HFD-fed *LCN2*$^{-/-}$ mice compared with wild-type control mice (Fig. 5*C*). Downregulation of *arginase* 1 and interleukin (*IL*)-*10* was also observed in the liver of HFD-fed *LCN2*$^{-/-}$ mice (Fig. 5*C*).

***LCN2*$^{-/-}$ mice develop dyslipidemia and fatty liver.** To investigate whether increased liver weight in *LCN2*$^{-/-}$ mice is associated with the development of fatty liver and dyslipidemia, liver triglyceride content and blood lipid profiles were measured. In comparison with wild-type controls, HFD-fed and aged *LCN2*$^{-/-}$ mice demonstrated a significant increase in lipid accumulation as detected by oil-red o staining of the liver section (Fig. 6*A*) and the increased levels of liver triglycerides (Fig. 6*B*). The development of more severe fatty liver disease, together with elevated fasting blood glucose levels, suggests hepatic insulin resistance in *LCN2*$^{-/-}$ mice. To elucidate hepatic glucose production in wild-type and LCN2-deficient mice fed an HFD, mice were fasted for 18 h and gene expression of two key gluconeogenic enzymes PEPCK and glucose-6-phosphatase (G6Pase) were detected by quantitative PCR. As illustrated in Fig. 6*C*, expression levels of *PEPCK1*, *PEPCK2*, and *G6Pase* genes were significantly higher in the liver of *LCN2*$^{-/-}$ mice than that in wild-type controls, suggesting that increased hepatic glucose production is attributed to hyperglycemia in *LCN2*$^{-/-}$ mice. We next examined the hepatic capabilities for fatty acid synthesis and oxidation to explore the possible mechanism for the

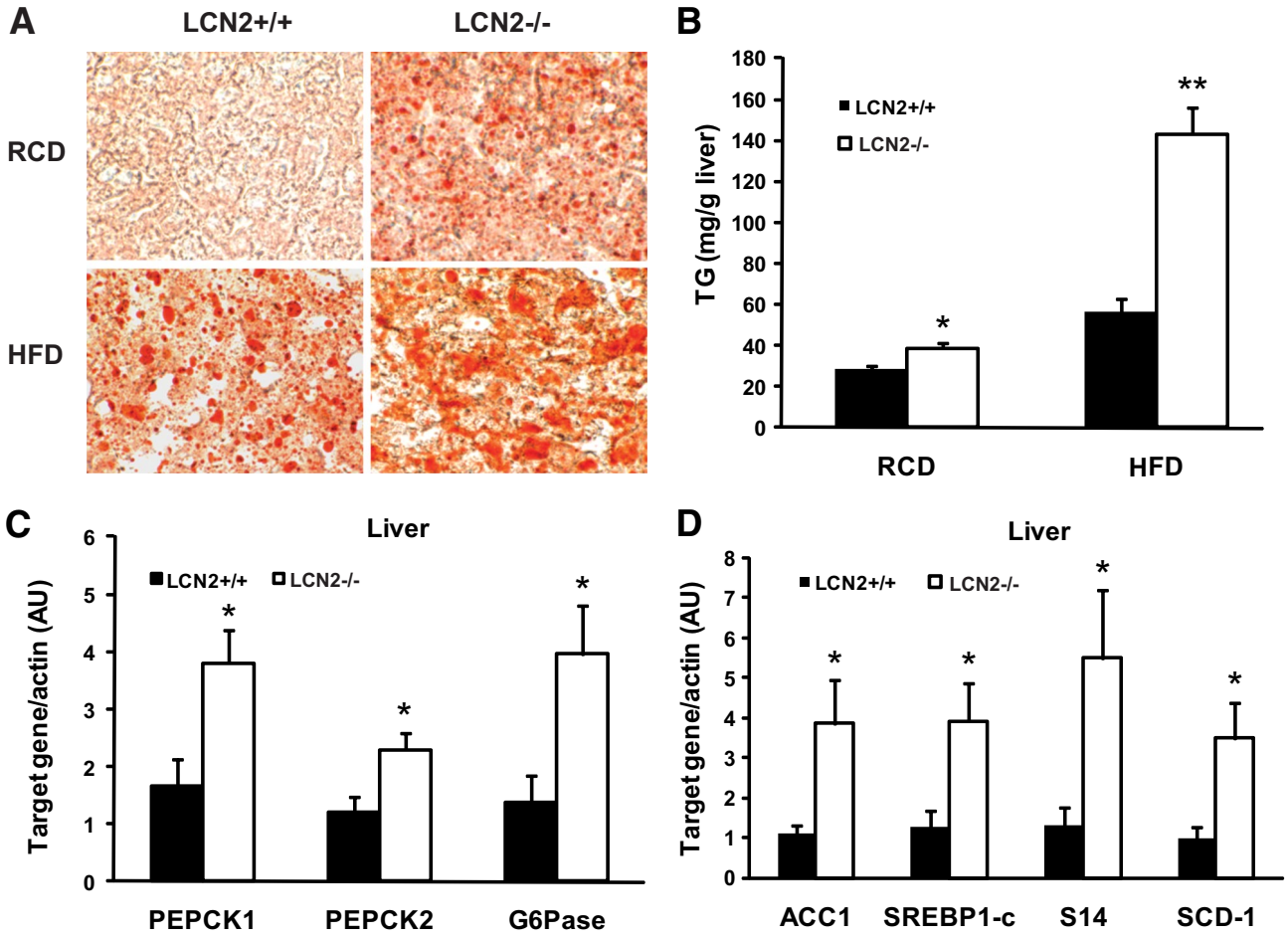

FIG. 6. Liver triacyglyceride content in *LCN2*$^{-/-}$ mice. *A*: Oil-red O staining of liver section of LCN2 $^{-/-}$ mice. *B*: Liver triacyglyceride levels in *LCN2*$^{-/-}$ mice on an RCD (n = 6–8, age 30 weeks) and an HFD (n = 11, age 15–16 weeks). *C*: The mRNA expression of gluocneogenic genes in liver (n = 6). *D*: The mRNA expression of lipogenic genes in liver (n = 6). The data are represented as means ± SE. *P < 0.05; **P < 0.01. (A high-quality digital color representation of this figure is available in the online issue.)

development of fatty liver in *LCN2*$^{-/-}$ mice. As illustrated in Fig. 6*D*, the lipogenic genes sterol regulatory element-binding protein-1c (*SREBP-1c*), acetyl-CoA carboxylase 1 (*ACC1*), Spot 14 (*S14*), and *SCD-1* were expressed at a significantly higher level in HFD-fed *LCN2*$^{-/-}$ mice compared with wild-type controls, while genes involved in fatty acid oxidation such as *PPARα*, *CPT*-1, and acetyl-CoA carboxylase 2 were similarly expressed between genotypes (data not shown). Therefore, the development of fatty liver results primarily from the increased capability for fatty acid synthesis in the liver in *LCN2*$^{-/-}$ mice.

Blood lipid profiles are summarized in Table 2. Compared with wild-type mice, *LCN2*$^{-/-}$ mice on an RCD had significantly higher serum levels of triglycerides, cholesterol, and free fatty acids. The HFD feeding did not induce a further increase in serum levels of triglyceride and cholesterol but significantly augmented the levels of LDL and β-hydroxybutyrate in *LCN2*$^{-/-}$ mice compared with wild-type controls. The above data have suggested that LCN2-deficient mice became more insulin resistant upon HFD feeding and age. Since adipose tissue is a key site for insulin-regulated glucose/lipid metabolism and glucose disposal, we examined the expression of genes involved
in lipid metabolism in primary adipose cells isolated from *LCN2*$^{-/-}$ mice. Compared with wild-type adipose cells, expression levels of genes involved lipid metabolism and adipokines, including *PPARγ*, lipoprotein lipase

TABLE 2
Plasma lipid profile in wild-type and LCN2-null mice

Genotype	Diet	Triglycerides (mg/dl)	Cholesterol (mg/dl)	HDL direct (mg/dl)	LDL direct (mg/dl)	Nonesterified fatty acids (mEq/l)	β-Hydroxybutyrate (mmol/l)
Wild type	RCD	89.76 ± 3.39	168.14 ± 5.56	85.26 ± 3.59	7.07 ± 0.29	1.31 ± 0.03	0.36 ± 0.03
LCN2$^{-/-}$	RCD	100.07 ± 4.05	191.82 ± 6.17*	94.99 ± 4.75	6.71 ± 0.38	1.58 ± 0.07	0.27 ± 0.05
Wild type	HFD	110.23 ± 3.34	194.72 ± 4.59	90.5 ± 2.23	6.74 ± 0.33	1.23 ± 0.07	0.39 ± 0.04
LCN2$^{-/-}$	HFD	99.34 ± 1.78	197.26 ± 14.82	86.63 ± 2.79	17.38 ± 3.19†	1.11 ± 0.04	0.48 ± 0.02†

Data are means ± SE. Measurements were performed on 6-h–fasted mice fed an RCD and HFD (n = 9–11). *P < 0.01 vs. wild-type on an RCD; †P < 0.01 vs. wild-type on an HFD.

(*LPL*), *GLUT4*, adiponectin, and leptin were markedly reduced in adipose tissue of HFD-fed *LCN2*$^{-/-}$ mice (online appendix Fig. S2).

DISCUSSION

We show here that LCN2 plays a critical role in lipid metabolism, adaptive thermoregulation, and diet-induced obesity and insulin resistance in vivo. Lack of LCN2 in mice potentiates HFD-induced obesity, dyslipidemia, fatty liver, glucose intolerance, and insulin resistance. We also discovered that LCN2 is a critical regulator of adaptive thermogenesis and mitochondrial oxidative function in BAT. LCN2 deficiency impairs adaptive thermogenesis and increases the susceptibility of *LCN2*$^{-/-}$ mice to HFD-induced obesity.

Our data demonstrated that *LCN2*$^{-/-}$ mice gained more body weight when they were fed HFD or aged. Increased body fat mass together with enlarged multiple organs may contribute to the development of higher body weight in *LCN2*$^{-/-}$ mice. In particular, increased organ weights may largely account for increased body weight in *LCN2*$^{-/-}$ mice under the RCD condition. In general, wild-type and *LCN2*$^{-/-}$ mice at a young age did not demonstrate significantly different metabolic phenotypes when they were fed RCD. However, *LCN2*$^{-/-}$ mice developed more severe systemic insulin resistance, hyperglycemia, hyperinsulinemia, and hypoadiponectinemia under the HFD condition. One of the most profound phenotypic features of *LCN2*$^{-/-}$ mice is cold sensitivity and lower body temperature under thermal stress conditions. It has been known for a long time that nonshivering thermogenesis is used to maintain constant body temperature and energy balance, controlling body weight, especially in small mammals (17–19). Both neural and hormonal signals, including norepinephrine, epinephrine, thyroid hormones, glucagon, insulin, glucocorticoid, and leptin, are known to regulate thermogenesis (17,20) through different thermogenic mechanisms involving stimulating ATP utilization, increasing UCP-1–mediated proton leak and heat production and affecting substrate availability and utilization for energy production. In rodents, BAT is the main tissue that is responsible for sympathetic nervous system–regulated nonshivering themogenesis with the involvement of norepinephrine and epinephrine (17,20,21). *UCP-1* and *PGC-1α* are the key genes that mediate sympathetic thermogenic responses in BAT. Low sympathetic activity is known to be associated with obesity (22). For example, *UCP-1* gene expression in BAT of *ob/ob* mice was reduced (23). However, BAT *UCP-1* expression could be normally stimulated in response to cold environment in young *ob/ob* mice, albeit *ob/ob* mice show decreased capability of utilizing fat and cold intolerance (23).

In this study, we found that 5-h cold exposure leads to a significant increase in LCN2 expression in WAT, which is in agreement with the result in a recent study (24). In the absence of LCN2, mice were cold intolerant and failed to maintain the body temperature when acutely exposed to cold temperature. Interestingly, cold exposure could still significantly stimulate gene expression of *UCP-1* and *PGC-1α* in BAT in *LCN2*$^{-/-}$ mice, suggesting that cold-induced sympathetic thermogenesis remained intact in the absence of LCN2. The role of leptin in thermogenesis has been well documented, and its thermogenic effect is considered to be primarily central (25). The peripheral role of leptin in thermogenesis is controversial. For example, leptin administration has been reported to rescue cold-induced hypothermia in the absence of UCP-1 in *leptin* and *UCP-1* double knockout mice (26,27), while the opposite results were perceived in the other two independent studies (28,29). In *LCN2*$^{-/-}$ mice on RCD, serum leptin levels were not different from that in wild-type mice, albeit serum leptin levels had a trend toward decreased in *LCN2*$^{-/-}$ mice in response to HFD feeding. Additionally, wild-type and *LCN2*$^{-/-}$ mice on an RCD did not exhibit a difference in body temperature in thermoneutral conditions. Our results suggest that the central control of body temperature may function normally. Therefore, it seems rather unlikely that leptin could be the major contributor to cold intolerance in *LCN2*$^{-/-}$ mice; leptin may be only partially involved in LCN2-regulated thermogenesis.

In addition to hormonal signals, defects in key metabolic regulators of substrate availability for energy production, ATP synthesis and mitochondrial biogenesis and oxidative function could all possibly affect thermogenic function. Indeed, studies in mice with the genetic disruption of key metabolic regulators have proved this assumption; mice without expressing ATGL could similarly result in cold intolerance (30). In the present study, the disruption of LCN2 completely diminished cold-induced *HSL* gene expression in BAT and WAT, whereas ATGL expression in WAT was only slightly affected in *LCN2*$^{-/-}$ mice under both the HFD and cold conditions. Since *HSL*$^{-/-}$ mice are not cold sensitive (31), HSL is not an important regulator for adaptive thermogenesis. Therefore, the effect of changes in ATGL levels on the supply of substrates for energy production for thermogenesis is minimal in *LCN2*$^{-/-}$ mice. On the other hand, the production of the energy necessary for thermogenesis requires normal mitochondrial oxidative function, and mitochondrial dysfunction could have a significant impact on adaptive thermogenesis. This hypothesis has been supported by a previous study in estrogen-related receptor α (EERα) knockout mice. In EERα-deficient mice, mitochondrial biogenesis and oxidative function in BAT was disturbed, and mice failed to maintain body temperature when exposed to cold (32). To this end, we further investigated the mitochondrial oxidative capacity of BAT and skeletal muscle. Interestingly, we found that the expression levels of mitochondrial genes involved in mitochondrial biogenesis and oxidative function such as *Nrf1*, *Tfam*, *ATP5b*, *COX 4*, and *CPT-1β* were significantly reduced in BAT of *LCN2*$^{-/-}$ mice fed an HFD. In the skeletal muscle, the expression of β-oxidation genes *PPARδ* and *CPT-1*, as well as mitochondrial genes *Nrf1* and *Tfam*, were also downregulated in HFD-fed *LCN2*$^{-/-}$ mice.

All the above data together suggest that mitochondrial metabolism is dysfunctional in BAT and muscle of *LCN2*$^{-/-}$ mice, which mainly contributes to decreased thermogenic capacity, decreased energy expenditure, and the high susceptibility to diet-induced obesity and insulin resistance during the thermal stress conditions (mice have been living at 22°C). In acute cold, muscle-shivering thermogenesis is considered to be the primary mechanism for a body temperature defense (21,33,34). BAT nonshivering thermogenesis participates in combating the cold temperature only when the extra capacity is already recruited for using during the acute cold exposure (35). Therefore, cold intolerance (acute exposure to 4°C for 5 h) in *LCN2*$^{-/-}$ mice may largely result from decreased oxidative capacity in skeletal muscle and BAT as well as decreased ATGL expression in WAT.

Our results clearly demonstrated that insulin responsiveness in muscle, adipose tissue, and liver was reduced, indicating systemic insulin resistance in *LCN2*$^{-/-}$ mice. Furthermore, fasting for 18 h induces significantly higher levels of expression for *PEPCK* and *G6Pase* in the liver of HFD-fed *LCN2*$^{-/-}$ mice, supporting that the increased hepatic glucose production is an important contributor to fasting hyperglycemia in *LCN2*$^{-/-}$ mice. Dyslipidemia such as hypertriacylglycerolemia and hypercholesterolemia is another prominent feature perceived in *LCN2*$^{-/-}$ mice. This phenomenon is likely due to the impaired regulation of lipid metabolism in adipose tissue and liver in *LCN2*$^{-/-}$ mice. We showed that *LCN2*$^{-/-}$ mice on an RCD had higher serum levels of triglycerides but lower serum triglyceride levels when fed an HFD as compared with wild-type mice. Lower serum triglycerides in HFD-fed *LCN2*$^{-/-}$ mice could be due to the increased triglycerides synthesis and decreased VLDL (or triglyceride) secretion into the circulation resulting from the development of fatty liver in *LCN2*$^{-/-}$ mice. This explanation is strengthened by a previous study (36) in LIRKO (insulin receptor knockout) mice with hepatic insulin resistance and 50% decrease in serum triglyceride levels.

As reported in our previous in vitro study (6), LCN2 is capable of suppressing inflammatory response of macrophages to LPS stimulation. We speculated that LCN2 possesses anti-inflammatory role in metabolic regulation. In this in vivo study, we show that LCN2 expression is downregulated in adipose tissue and bone marrow macrophages (BM-MAC) in HFD-induced obese mice. In the absence of LCN2, the expression of proinflammatory cytokines such as MCP-1 and TNFα are upregulated in adipose tissue, while expression levels of anti-inflammatory markers arginase 1 and IL-10 are decreased in adipose tissue and liver, suggesting an increased inflammatory state in *LCN2*$^{-/-}$ mice. These results further suggest that *LCN2*$^{-/-}$ mice are more susceptible to HFD-induced proinflammatory response than wild-type mice.

In summary, herein we discovered a novel role for LCN2 in energy metabolism, adaptive thermogenesis, and insulin resistance. Mice lacking LCN2 display impaired adaptive thermogenesis and deteriorated diet-induced obesity and insulin resistance. Decreased mitochondrial oxidative capacity in BAT and skeletal muscle may be the primary mechanisms for the development of diet-induced insulin resistance and cold sensitive in *LCN2*$^{-/-}$ mice. However, the mechanisms for how LCN2 regulates mitochondrial function and lipid metabolism remain to be further identified. It is likely that the binding of LCN2 to small hydrophobic molecules such as retinoic acids, fatty acids, and other unknown ligands or to the cell surface receptor such as megalin or LDL-related protein 2 (37) could potentially involve or mediate LCN2 effects in metabolism. Our findings provide new insight into the role of LCN2 in lipid metabolism and metabolic homeostasis. In this manner, LCN2 may be a potential therapeutic target for controlling obesity-associated type 2 diabetes and metabolic complications.

ACKNOWLEDGMENTS

The project described was supported by grant no. R01DK080743 (to X.C.) from the National Institute of Diabetes and Digestive and Kidney Diseases.

No potential conflicts of interest relevant to this article were reported.

The content is solely the responsibility of the authors and does not necessarily represent the official views of the National Institute of Diabetes and Digestive and Kidney Diseases or the National Institutes of Health. We thank Mark Sanders from Imaging Center at the University of Minnesota for technical assistance in liver oil-red O staining and Dr. Doug Mashek and Mara Mashek from the Department of Food Science and Nutrition at the University of Minnesota for assistance in the measurement of liver triacylglyceride.

REFERENCES

1. Attie AD, Scherer PE. Adipocyte metabolism and obesity. J Lipid Res 2009;50 (Suppl.):S395–S399
2. Badman MK, Flier JS. The adipocyte as an active participant in energy balance and metabolism. Gastroenterology 2007;132:2103–2115
3. Hotamisligil GS. Inflammation and metabolic disorders. Nature 2006;444: 860–867
4. Rosen ED, Spiegelman BM. Adipocytes as regulators of energy balance and glucose homeostasis. Nature 2006;444:847–853
5. Yan QW, Yang Q, Mody N, Graham TE, Hsu CH, Xu Z, Houstis NE, Kahn BB, Rosen ED. The adipokine lipocalin 2 is regulated by obesity and promotes insulin resistance. Diabetes 2007;56:2533–2540
6. Zhang J, Wu Y, Zhang Y, Leroith D, Bernlohr DA, Chen X. The role of lipocalin 2 in the regulation of inflammation in adipocytes and macrophages. Mol Endocrinol 2008;22:1416–1426
7. Kjeldsen L, Johnsen AH, Sengelov H, Borregaard N. Isolation and primary structure of NGAL, a novel protein associated with human neutrophil gelatinase. J Biol Chem 1993;268:10425–10432
8. Kjeldsen L, Bainton DF, Sengelov H, Borregaard N. Identification of neutrophil gelatinase-associated lipocalin as a novel matrix protein of specific granules in human neutrophils. Blood 1994;83:799–807
9. Cowland JB, Borregaard N. Molecular characterization and pattern of tissue expression of the gene for neutrophil gelatinase-associated lipocalin from humans. Genomics 1997;45:17–23
10. LaLonde JM, Bernlohr DA, Banaszak LJ. The up-and-down beta-barrel proteins. FASEB J 1994;8:1240–1247
11. Yang Q, Graham TE, Mody N, Preitner F, Peroni OD, Zabolotny JM, Kotani K, Quadro L, Kahn BB. Serum retinol binding protein 4 contributes to insulin resistance in obesity and type 2 diabetes. Nature 2005;436:356–362
12. Flo TH, Smith KD, Sato S, Rodriguez DJ, Holmes MA, Strong RK, Akira S, Aderem A. Lipocalin 2 mediates an innate immune response to bacterial infection by sequestrating iron. Nature 2004;432:917–921
13. Bligh EG, Dyer WJ. A rapid method of total lipid extraction and purification. Can J Biochem Physiol 1959;37:911–917
14. Xiang CC, Wu YJ, Ma L, Ding L, Lisinski I, Brownstein MJ, Cushman SW, Chen X. Characterisation of insulin-resistant phenotype of cultured rat primary adipose cells. Diabetologia 2007;50:1070–1079
15. Weber, TM, Joost, HG, Simpson IA, Cushman SW *The Insulin Receptor*. New York, A.R. Liss, 1988
16. Hirsch J, Knittel JL. Cellularity of obese and non-obese human adipose tissue. Fed Proc 1970;29:1516–1521
17. Jansky L. Humoral thermogenesis and its role in maintaining energy balance. Physiol Rev 1995;75:237–259
18. Lowell BB, Spiegelman BM. Toward a molecular understanding of adaptive thermogenesis. Nature 2000;404:652–660
19. Spiegelman BM, Flier JS. Obesity and the regulation of energy balance. Cell 2001;104:531–543
20. Silva JE. Thermogenic mechanisms and their hormonal regulation. Physiol Rev 2006;86:435–464
21. Cannon B, Nedergaard J. Brown adipose tissue: function and physiological significance. Physiol Rev 2004;84:277–359
22. Bray GA, York DA. The MONA LISA hypothesis in the time of leptin. Recent Prog Horm Res. 1998;53:95–117; [discussion 117–118]
23. Jacobsson A, Stadler U, Glotzer MA, Kozak LP. Mitochondrial uncoupling protein from mouse brown fat. molecular cloning, genetic mapping, and mRNA expression. J Biol Chem 1985;260:16250–16254
24. Roudkenar MH, Halabian R, Roushandeh AM, Nourani MR, Masroori N, Ebrahimi M, Nikogoftar M, Rouhbakhsh M, Bahmani P, Najafabadi AJ, Shokrgozar MA. Lipocalin 2 regulation by thermal stresses: Protective role of Lcn2/NGAL against cold and heat stresses. Exp Cell Res 2009;315:3140–3151
25. Margetic S, Gazzola C, Pegg GG, Hill RA. Leptin: a review of its peripheral actions and interactions. Int J Obes Relat Metab Disord 2002;26:1407–1433

26. Ukropec J, Anunciado RP, Ravussin Y, Hulver MW, Kozak LP. UCP1-independent thermogenesis in white adipose tissue of cold-acclimated Ucp1$^{-/-}$ mice. J Biol Chem 2006;281:31894–31908
27. Ukropec J, Anunciado RV, Ravussin Y, Kozak LP. Leptin is required for uncoupling protein-1-independent thermogenesis during cold stress. Endocrinology 2006;147:2468–2480
28. Commins SP, Watson PM, Frampton IC, Gettys TW. Leptin selectively reduces white adipose tissue in mice via a UCP1-dependent mechanism in brown adipose tissue. Am J Physiol Endocrinol Metab 2001;280:E372–E377
29. Okamatsu-Ogura Y, Uozumi A, Toda C, Kimura K, Yamashita H, Saito M. Uncoupling protein 1 contributes to fat-reducing effect of leptin. Obes Res Clin Pract 2007;1:233–241
30. Haemmerle G, Lass A, Zimmermann R, Gorkiewicz G, Meyer C, Rozman J, Heldmaier G, Maier R, Theussl C, Eder S, Kratky D, Wagner EF, Klingenspor M, Hoefler G, Zechner R. Defective lipolysis and altered energy metabolism in mice lacking adipose triglyceride lipase. Science 2006;312:734–737
31. Osuga J, Ishibashi S, Oka T, Yagyu H, Tozawa R, Fujimoto A, Shionoiri F, Yahagi N, Kraemer FB, Tsutsumi O, Yamada N. Targeted disruption of hormone-sensitive lipase results in male sterility and adipocyte hypertrophy, but not in obesity. Proc Natl Acad Sci U S A 2000;97:787–792
32. Villena JA, Hock MB, Chang WY, Barcas JE, Giguere V, Kralli A. Orphan nuclear receptor estrogen-related receptor alpha is essential for adaptive thermogenesis. Proc Natl Acad Sci U S A 2007;104:1418–1423
33. Griggio MA. The participation of shivering and nonshivering thermogenesis in warm and cold-acclimated rats. Comp Biochem Physiol A Comp Physiol 1982;73:481–484
34. Block BA. Thermogenesis in muscle. Annu Rev Physiol 1994;56:535–577
35. Rothwell NJ, Stock MJ. Similarities between cold- and diet-induced thermogenesis in the rat. Can J Physiol Pharmacol 1980;58:842–848
36. Biddinger SB, Hernandez-Ono A, Rask-Madsen C, Haas JT, Aleman JO, Suzuki R, Scapa EF, Agarwal C, Carey MC, Stephanopoulos G, Cohen DE, King GL, Ginsberg HN, Kahn CR. Hepatic insulin resistance is sufficient to produce dyslipidemia and susceptibility to atherosclerosis. Cell Metab 2008;7:125–134
37. Devireddy LR, Teodoro JG, Richard FA, Green MR. Induction of apoptosis by a secreted lipocalin that is transcriptionally regulated by IL-3 deprivation. Science 2001;293:829–834